Preliminary results from a Monte Carlo study of breast tumour imaging with a low energy high resolution collimator and a modified uniformly redundant array coded aperture

M. Alnafea[a], K. Wells[a*], N.M. Spyrou[a], M.I Saripan[a], M. Guy[b], P. Hinton[b]

[a]*School of Electronics & Physical Sciences, University of Surrey, Guildford, Surrey, GU2 7XH, UK*

[b]*Department of Nuclear Medicine, Royal Surrey County Hospital, Guildford, Surrey, GU2 7XX, UK*

* corresponding author

email k.wells@eim.surrey.ac.uk. Phone +44 1483 686036. FAX +44 1483 686031

Abstract

This paper considers Scintimammography (SM) imaging using two different image acquisition/formation methods: Low Energy High Resolution (LEHR) collimator and a Modified Uniformly Redundant Array (MURA) coded aperture (CA) systems. Using Monte Carlo simulation, the effectiveness and performance of both systems were evaluated by quantitative comparison of lesion contrast and Full-Width-Half-Maximum under a variety of clinical imaging situations. The results from the CA studies suggest that for the particular geometry studied, the MURA-CA gives comparable performance compared to using a LEHR collimator.

Keywords:

Coded aperture imaging; Scintimammography; Monte Carlo simulation; phantom study; Breast tumour imaging; MURA

1. Introduction

Scintimammography (SM) performed with a gamma camera (most often employing ^{99m}Tc labeled Sestamibi) has been studied with significant interest over recent years. This technique produces a range of different imaging approaches such as single photon emission computed tomography (SPECT) with elliptical orbits [1], and planar imaging (with and without breast compression) [2]. These results suggest that a radionuclide approach to breast tumor imaging can have significant diagnostic value [3], stimulating the development of small dedicated high resolution gamma camera instrumentation [4-6]. However, collimator-based γ-ray imaging systems utilize a very small fraction, ~ 0.1-0.01%, of the total number of the emitted photons. This means that the collimator tends to be the limiting factor for both system spatial resolution and sensitivity. By contrast, this study focuses on planar SM comparing two different methods: a Low Energy High Resolution (LEHR) collimator and Modified Uniformly Redundant Array (MURA) [7] Coded Aperture (CA) systems in order to explore whether a CA with a standard clinical gamma camera can be used in such an application. The imaging performance of both LEHR collimator and CA imaging were measured by considering two fundamental parameters: lesion contrast and FWHM under a variety of idealized and clinically realistic imaging conditions.

2. Monte Carlo simulation code description

2.1. Simulated Geometry using MCNPX

Monte Carlo N-Particle eXtended (MCNPX version 2.4.0) as used in this study, is a 3D general-purpose radiation transport code [8] that provides an accurate physics simulation within the photon range encountered in nuclear medicine imaging [9]. Figure 1 shows the different elements of the complete geometry studied for the two proposed systems. Spherical sources representing tumors are located inside the breast, with a uniform background activity assigned to the surrounding media. We considered only ^{99m}Tc isotropic sources emitting 140 keV photons. The upper body torso phantom was represented by a parallelepiped of 40x40x20 cm^3 filled with tissue equivalent material. All tissue atomic compositions were taken from the ICRU report 44 [10].

The breast is represented as semi-compressed to a thickness of 6cm, with a projected area of 20x20 cm^2. We assume the breast material density is similar to that found in the uncompressed breast. The tumor (5 or 10mm diameter sphere) was positioned at 3cm depth from the surface of the breast and the centre of lesion to front of collimator (or CA) distance is always 7cm (and 30cm respectively).

In the initial geometry of CA SM we utilize a MURA pattern [7] of 241x241 element array (dimension 24.1 x 24.1 cm^2) placed midway (see Fig. 1) between the tumor central plane and the front surface of the camera by 60cm. Thus, the magnification factor was 1 and the simulated mask material is 1.5 mm thick tungsten, which corresponds to ~99% attenuation for normal incidence 140 keV photons; the unit hole-size of the mask is a square of 1x1mm^2. This configuration of MURA geometry is used to cover the field of view. The raw projected (encoded) image is decoded by using correlation with a binary array representing the coded aperture [7]. In the second part of the work, the CA mask was then removed and a LEHR collimator placed in close proximity to the NaI crystal, with a 7cm distance between lesion centre and collimator face. In this case the raw projection images were used for assessment.

Photons are generated either in the background object or the lesions under study. The resulting photon histories track individually, the positions of interactions and energy losses that are then recorded in a single output list file, referred to as a PTRAC file [8].

A simple post-processing program was written in-house to extract those histories (from the PTRAC ASCII file) corresponding to photons which interacted in the gamma camera's NaI crystal. These are then subject to the effects of the gamma camera's limited photoelectron statistics reflected in the finite energy and spatial resolution. To account for these effects, we have utilized experimental values derived from a-priori experiments using a Toshiba GCA7100A gamma camera. The data are stochastically blurred with a Gaussian point spread function with FWHM=3.7mm corresponding to the intrinsic spatial resolution of the aforementioned Toshiba camera. Backscatter from the photomultiplier tube array is approximated by following the method recommended by [11]. An acceptance window defined by 20% about the peak energy (140 keV), as used in clinical practice, is used to reject photons which fall outside this window. Further details and validation of the camera simulation appear elsewhere [12].

2.2. Activity calculation

For a clinically realistic Monte Carlo simulation in the cranio-caudal view, the number of simulated gamma rays must be comparable to that obtained in a typical imaging study. As reported in [13] the patient is typically injected with ~ 20 mCi (740 MBq) of ^{99m}Tc-sestamibi and imaged for 10 minutes. It is assumed, to first order, that the distribution of radioactivity in the torso is uniform. Based upon the branching ratio for ^{99m}Tc (approximately 89%), ignoring the small decay loss before and during the scan and adjusting for omissions in the simulated phantom geometry (e.g. no liver, lungs, legs, head, or bladder present) then the total estimated number of emitted photons during the scan is ~ 10^{11} photons emitted over 10 minutes.

We define a sphere within the torso of 8cm diameter corresponding to the heart. This commonly has a significantly higher activity concentration than most other non-tumor tissues, due to its substantial blood supply and the fact that Sestamibi is a heart imaging agent. A heart-background-ratio of 10:1 is assumed based on [6]. Tumor activity to background ratio (TBR) concentration in the simulations is then varied ranging from 3:1 up to 100:1 for 5 and 10mm tumor diameters shown in table 1. This demonstrates the extremely low integrated flux available for small lesions at low TBR.

3. Simulation results and discussion

We now consider the resolution and contrast observed for both different lesion sizes and different TBR uptake.

3.1. Resolution

In SM, tumor FWHM reveals the system's susceptibility to projected partial volume effects in the 2D planar image in the presence of limited signal and statistical noise. Each FWHM reported in Fig. 2 was calculated based on the average of vertical, horizontal and diagonal profiles drawn through the centre of the detected tumor after a Gaussian curve fit to the data. Fig. 2 demonstrates that both geometries give very similar results.

Note that for the LEHR collimator, the 5mm & 10 mm diameter tumour with TBRs of 3, 5, and 10 were not visualized and it become impossible to calculate FWHM or contrast.. In this case lesion visibility is seriously degrade by the cardiac flux and unwanted (unrelated) activity in the torso. In the case of the coded aperture the 5mm diameter tumour was not visualized (with any TBR). The 10 mm diameter tumour was also not visualized at any TBR less than 20.

3.2. Contrast

Lesion contrast was used to quantify the lesion visibility. The contrast *(C)* is defined by normalizing the tumour signal *(S)* to the background *(B)* as:

$$C = \frac{S - B}{B} \qquad \ldots\ldots 1$$

The signal was obtained using a region of interest (ROI) that is defined by the FWHM. For the CA geometry, the 5mm diameter tumour was not visualized with any TBR simulated. However for a 10 mm lesion with TBR > 20 the contrast is lower compared to LEHR collimator. Non-specific torso activity significantly affects contrast for the CA system, which may be attributed to the open aperture nature of the system. This suggests careful

shielding of cardiac and other unrelated activity will be important aspects of CA system design. However, for the LEHR collimator system and a 10 mm lesion with TBR > 20, the contrast is higher compared to the coded aperture. The improvement in contrast varies up to double that of the CA system, as shown in Fig. 2.

4. Conclusion

We have described the application of both LEHR collimator and MURA-CA imaging system in SM. A range of TBRs has been investigated, from highly idealized TBRs of 100:1 to clinically realistic of TBRs of 5:1 and 3:1 for the two image formation methods. In this initial study, considering a realistic background activity distribution, and a variety of TBRs, we conclude that direct application of a MURA-CA in SM yields very similar overall performance, (albeit with reduced contrast), to LEHR collimator imaging when used for scintimammography imaging with a conventional gamma camera. However, the CA system is particularly sensitive to stray photons from outside the target ROI compared to collimator-based imaging, which has not been addressed in this preliminary report. New results where some of these factors have been considered, suggest a more promising performance for the CA system. We are thus undertaking an optimization of the coded-aperture approach that will be reported shortly [14].

Acknowledgments

We wish to thank D. Mahboub, A. Alghamdi and A. Ma for their valuable assistance and useful suggestions. We also thank and highly acknowledge the financial support from King Saud University, Saudi Arabia.

References

[1] A. Abufadel, et al., J Nucl Cardiol. 8 (2001) 458-465.

[2] R. Pani, et al., Anticancer Research 17 (1997) 1645-1649.

[3] I.N. Weinberg, et al., IEEE Trans. Nucl. Sci. 44 (1997) 1398.

[4] R. F. Brem , et al., Nucl. Instr. and Meth. A 497 (2003) 39.

[5] B. Mueller, et al., J. Nucl. Med. 44 (2003) 602-609.

[6] R. Pani, et al., IEEE Trans. Nucl. Sci. 45 (1998) 3127.

[7] S. R. Gottesman, & E.E. Fenimore Appl. Opt., (1989) 28, 4344

[8] J.F. Briesmeister, Ed., "MCNP - A General Monte Carlo N Particle Transport Code, Version 4B," LA-12625-M, 1997.

[9] H. Zaidi, Med. Phys. 26 (1999) 574.

[10] ICRU, Tissue Substitutes in Radiation Dosimetry and Measurement, Report 44 of the International Commission on Radiation Units and Measurements, 1989.

[11] D.J. de Vries et al., IEEE Trans. Med. Imaging 9 (1990) 430.

[12] M.I. Saripan, M. Alnafea, M. Petrou, K. Wells and M. Guy; Conference Proc. of Medical Image Understanding & Analysis Bristol, UK, 2005

[13] E. Bombardieri, et al., Eur. J. Nucl. Med. Mol. Imaging. 30 (2003) BP107–BP11.

[14] *M. Alnafea et al., presented at the 7th Position Sensitive Detector Conference, Liverpool, UK, Septmber 2005, and submitted to NIM A.*

Figure Captions

Figure 1: a schematic representation for the 3D torso phantom and MURA camera for Monte-Carlo simulation designed to emulate scintimammography. For CA simulations, X = 30cm. For the LEHR simulations the distance X = 7cm, where is the CA plane is removed and replaced by a LEHR collimator directly in front of the NaI (Tl) crystal.

Figure 2: The calculated tumour FWHM and contrast values calculated from 2D Monte Carlo simulations images of a 10 mm lesion as a function of TBR.

Table Caption

Table 1: Summary of lesion diameters and the estimated integrate flux. The lesions were assumed to be spherical where the upper figure indicates the estimated activity concentration (kBq/cc) and the lower figure showing the corresponding integrated lesion flux for a 10 minutes imaging study with an injected activity of ~740 MBq (20 mCi).

Table 1

	Tumor-Background-Ratio of Tissue Uptake						
	3 : 1	5 : 1	10 : 1	20 : 1	40 : 1	60 : 1	100 : 1
Tumor Activity	kBq/cc	kBq/cc	kBq/cc	kBq/cc	kBq/cc	kBq/cc	kBq/cc
Integrated Flux	γ	γ	γ	γ	γ	γ	γ
5 mm Tumor Diameter (mm)	2.17E+02	3.61E+02	7.22E+02	1.44E+03	2.89E+03	4.33E+03	7.22E+03
	8.51E+06	1.42E+07	2.84E+07	5.67E+07	1.13E+08	1.70E+08	2.84E+08
10 mm Tumor Diameter (mm)	2.17E+02	3.61E+02	7.22E+02	1.44E+03	2.89E+03	4.33E+03	7.22E+03
	6.81E+07	1.13E+08	2.27E+08	4.54E+08	9.08E+08	1.36E+09	2.27E+09

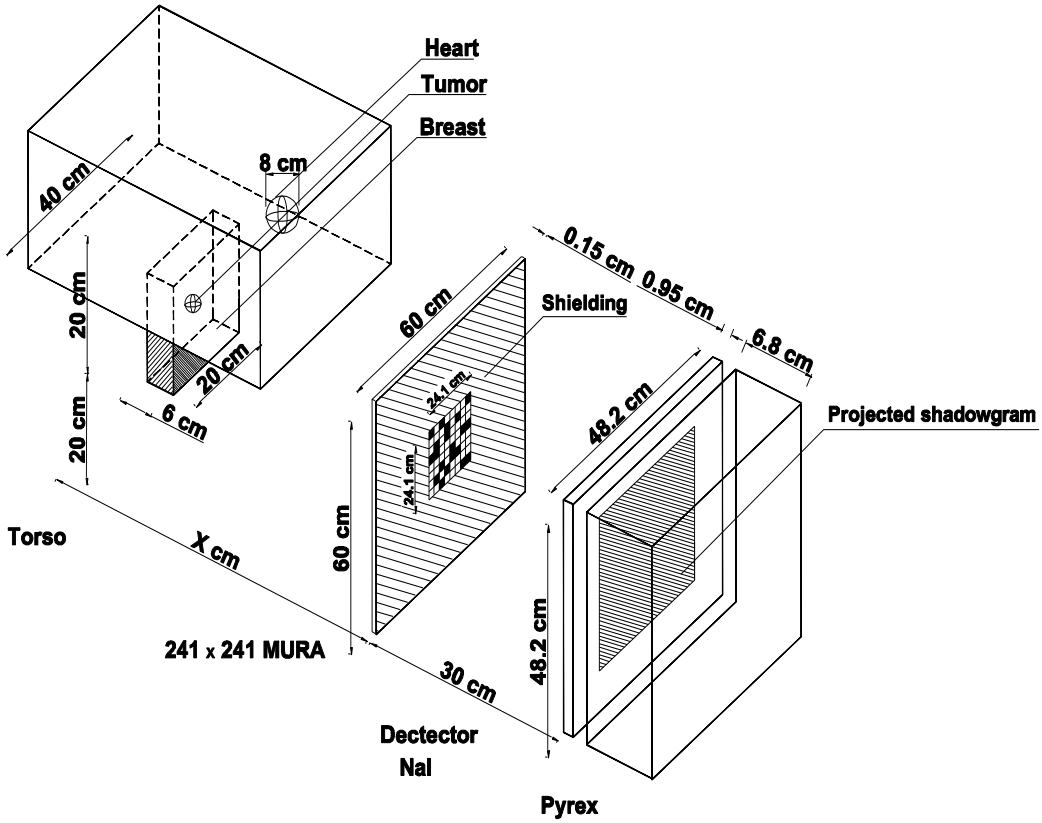
Heart
Tumor
Breast
8 cm
40 cm
20 cm
20 cm
20 cm
6 cm
60 cm
Shielding
0.15 cm
0.95 cm
6.8 cm
24.1 cm
24.1 cm
48.2 cm
Projected shadowgram
Torso
X cm
60 cm
241 x 241 MURA
30 cm
48.2 cm
Dectector
NaI
Pyrex

Fig. 1

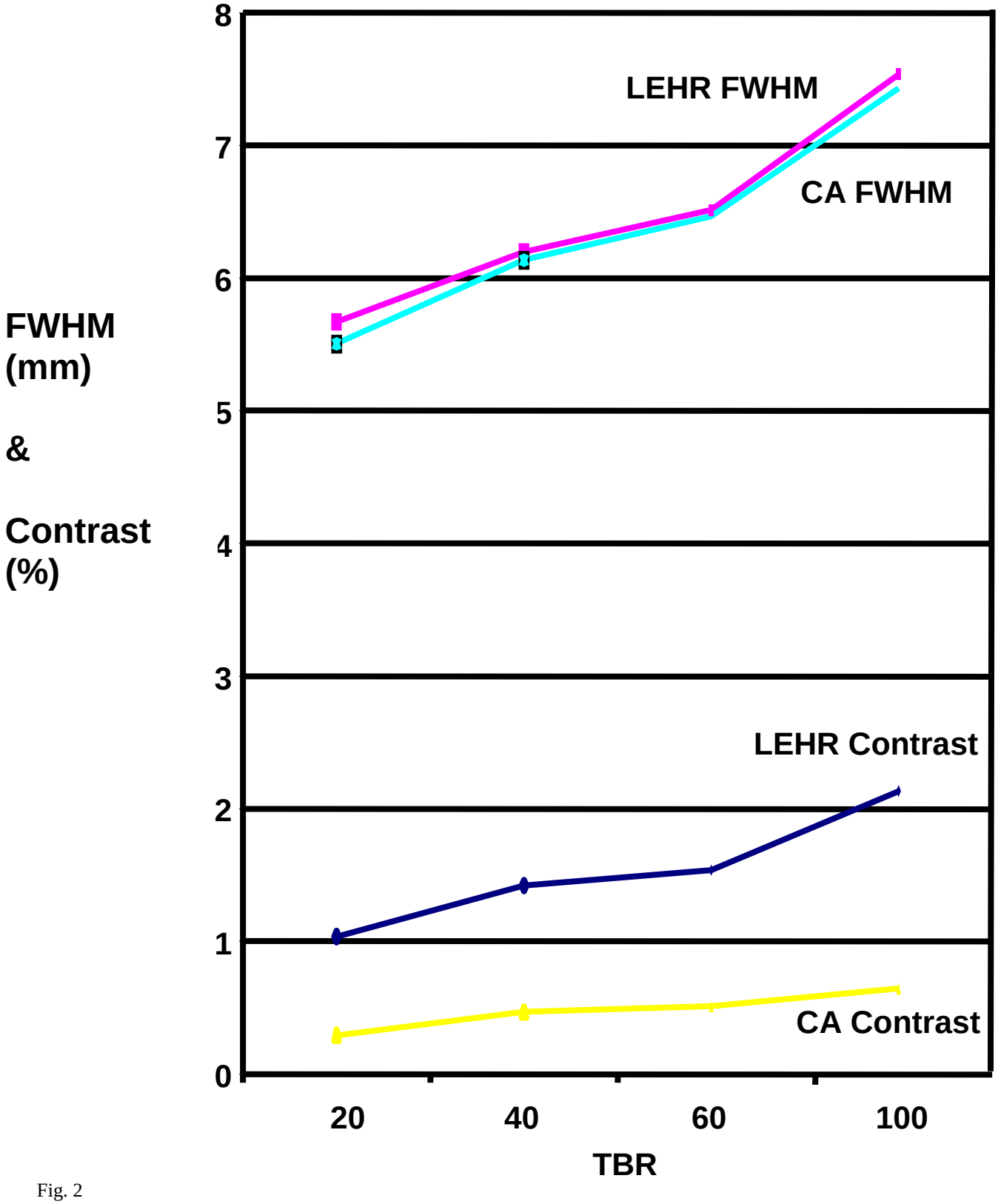
FWHM (mm) & Contrast (%)
8
7
6
5
4
3
2
1
0
LEHR FWHM
CA FWHM
LEHR Contrast
CA Contrast
20
40
60
100
TBR

Fig. 2